Combinatorial Library of Ternary Polyplexes Enables Identification of Improved siRNA Nanocarriers for Rapid In Vivo Translation

By:

Thomas A. Werfel

Thesis

Submitted to the Faculty of the

Graduate School of Vanderbilt University

in partial fulfillment of the requirements

for the degree of

Master of Science

in

Biomedical Engineering

May, 2015

Nashville, Tennessee

Approved:

Craig L. Duvall, Ph.D.

Todd D. Giorgio, Ph.D.

ACKNOWLEDGEMENTS

I must begin by thanking my advisor, Dr. Craig Duvall, who has laid the foundation for the work I am able to do and whose guidance is constantly elevating this work. Dr. Duvall has always been a "player's coach", advocating for his students and providing an atmosphere which drives us toward success without making our tasks all-consuming. Moreover, Dr. Duvall never lets his students settle and is always driving us toward the attainment of higher goals. This attribute is noticeably present throughout his publication record. I must thank all the amazing members of Dr. Duvall's Advanced Therapeutics Laboratory at Vanderbilt University for their support and comradery. Particularly, I thank Drs. Hongmei Li and Chris Nelson. Dr. Li, as she was the first to train me as a scientist and whose mentorship initiated my interest in research. Dr. Nelson, as his admirable work and ideas serve as the basis for the current work being presented. I would like to thank the following direct contributors to the work herein presented: Martina Miteva, Taylor Kavanaugh, Kellye Kirkbride, Meredith Jackson, Rebecca Cook, Todd Giorgio, and Craig Duvall. Thank you to Rene Colehour and Sarah Satterwhite who first introduced me to the great family here at Vanderbilt and who continue to stay in touch. Thank you to Dan Balikov for many meals and coffees and the great conversations which accompanied and helped to strengthen us through graduate school. Thank you to Ashton Werfel, my wife and the love of my life, for her continued support and constant grace as I pursue a career in science.

I am grateful to the Vanderbilt Institute for Nanoscale Science and Engineering (VINSE) for access to DLS and TEM (NSF EPS 1004083) for polyplex characterization. This work was supported by the Vanderbilt School of Engineering, the NIH through the grant NIH R21EB012750, the DOD through the grant CDMRP OR130302, and the NSF through the NSF GRFP #1445197.

TABLE OF CONTENTS

LIST OF FIGURES

Chapter I

Polymer Micelles / Polyplexes for Gene Therapy

Gene therapies have emerged as a part of the revolution in cell and molecular biology over the second half of the 20th century. While viral gene therapies represent the gold standard in terms of efficiency, therapeutic use of viruses remains shadowed by concerns with safety. Due to the tremendous opportunity for gene therapies to impact medicine, there is great motivation to work toward safer and targeted viral vectors and to also carry out parallel efforts toward engineering more efficient nonviral systems that can achieve safe, efficacious gene therapy in humans. Many of the recent breakthroughs in nonviral gene therapy are a result of advances in materials science, chemistry, and engineering that have enabled the synthesis/fabrication of more homogeneous materials with an array of well-defined and tunable functionalities, in addition to the evolution of technologies for more rigorous characterization of chemical composition and biological interactions of nanomaterials. Taken together, rapid advances in materials synthesis and characterization, combined with tremendous progress in our ability to manipulate the genome and molecular-level and nanoscale phenomena, are predicted to yield clinically-relevant breakthroughs in nonviral gene therapies that provide new and improved treatments for some of our most challenging diseases.

Nucleic acid-based drugs are sought for the replacement of missing, mutated, or deficient genes and for the suppression of gene expression by RNA interference (RNAi). Common classes of nucleic acid-based drugs include plasmid DNA (pDNA), messenger RNA (mRNA), short interfering RNA (siRNA), short hairpin RNA (shRNA), microRNA (miRNA), miRNA inhibitors, peptide nucleic acids (PNA), RNA-based adjuvants, and clustered regularly interspaced short

palindromic repeats/Cas (CRISPR/Cas) gene editing systems. The most heavily investigated delivery strategies are those for pDNA and siRNA delivery. Gene replacement/addition is the more mature field but comes with the extra challenges associated with delivering pDNA into the nucleus and the limitation that plasmids often do not stably integrate and thus do not have high potential for curing chronic genetic diseases. By contrast, RNAi by siRNA only requires delivery into the cytosol where the RNA-induced silencing complex (RISC) machinery is located. The activated RISC complex contains the antisense siRNA strand and mediates the recognition and subsequent enzymatic degradation of complementary mRNA. Both approaches require some common and disparate delivery considerations based on the desired intracellular pharmacokinetics. For instance, both require accumulation at the tissue compartment of interest and must cross the outer cell membrane. However, RNAi by siRNA will only require a carrier with endosomal escape mechanisms while gene augmentation/replacement achieved through delivery of pDNA requires intracellular trafficking into the nucleus.

In general, three major delivery barriers are considered when developing polymeric nanoparticles for gene therapy: 1) preferential biodistribution to the site of action, 2) cellular internalization by the targeted cell type, and 3) trafficking to and unpackaging within the intracellular compartment where the nucleic acid cargo will be active (Figure 1). Viruses have evolved mechanisms to efficiently overcome these barriers and are the inspiration for the design of biomimetic polymer nanoparticles. Continued breakthroughs in the elucidation of the mechanisms of action of viruses, combined with rapid advances in synthetic fabrication and characterization of virus-mimetic polymeric nanoparticles, suggests that more safe and effective nonviral gene therapies will continue to emerge.

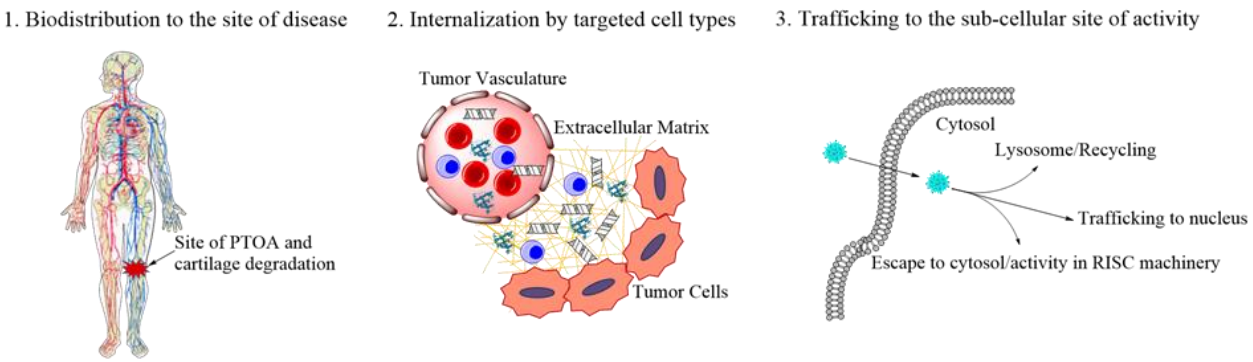

Figure 1. Schematic of the 3 major systemic and intracellular barriers to delivery of gene therapies. (1) The drug should be able to accumulate at the site of pathology, whether passively or by active targeting. (2) The drug should escape the circulation, navigate the ECM, and be internalized by the targeted cell types. (3) The drug should be trafficked to and released within the sub-cellular compartment where it is active.

A few major classes of polymeric nanoparticles such as micelles/polyplexes, cross-linked micelles, polymersomes, and nanogels have all been utilized for overcoming the above listed barriers to systemic drug delivery. Each class of polymer nanoparticle has strengths and shortcomings and the biomedical application will typically dictate choice of material as well as the potential for successful clinical translation. Herein, we focus upon gene and drug delivery from self-assembled micelles/polyplexes.

Micelles are self-assembling amphiphilic block copolymers with a core-shell (hydrophilic-hydrophobic) architecture. They are typically assembled in aqueous solutions by methods such as dialysis, pH adjustment, and dropwise addition of concentrated organic solutions. The formation of core-shell architecture is driven by entropic processes, resulting in segregation of a hydrophobic core from solution by a hydrophilic outer corona. This is an attractive architecture for drug delivery applications because it is possible to load hydrophobic small molecule therapeutics into the hydrophobic micelle core. The hydrophilic outer shell is often composed of PEG and serves as an aide for increased blood circulation and reduced cytotoxicity. In many gene therapy applications, the outer corona or the core are endowed with cationic functionalities that enable the electrostatic

packaging of nucleic acids. Pre-assembled micelles with a cationic corona can be used to load nucleic acids, forming "micelleplexes". In other approaches, a diblock polymer with one core-forming, cationic block and one neutral hydrophilic block (typically PEG) is assembled into PEGylated polyplexes, also known as polyion complex (PIC) micelles, upon mixing with anionic nucleic acid cargo. Physicochemical attributes such as size, shape, chemical composition, and charge are all important factors when considering the design of micelles as therapeutic carriers because they have profound effect on their effectiveness in overcoming in vivo delivery barriers.

The earliest approaches to using micelles/polyplexes as non-viral gene vectors employed cationic, amine-rich polymers such as poly(ethyleneimine) (PEI), poly(2-(dimethylamino)ethyl methacrylate) (PDMAEMA), and poly(L-lysine) (PLys). The amines of this class of cationic polymers are used for three purposes: 1) condensation/nuclease protection of negatively charged nucleic acids, 2) enhanced cellular uptake, and 3) endosomolytic escape. The positively charged amines form electrostatic interactions with and efficiently condense nucleic acids. The overall positive surface charge of the resulting particles also drives cellular uptake through mechanisms which are not yet fully elucidated, but which are likely mediated through anionic, heparin sulfate proteoglycans present on cell surfaces.[1, 2] After internalization, polymers with secondary and tertiary amines with pKa values at or just below pH 7 drive endosomolytic escape through the proton-sponge effect.[3, 4]

Polyplexes formed of solely of cationic homopolymers have shown promise as in vitro transfection agents but have many translational issues.[5] Their cationic charge causes cytotoxicity and limits their utility for systemic delivery. The cationic surface charge also causes aggregation with serum proteins and red blood cells, generally thought to be the reason for their eventual disproportionate accumulation in the capillary beds of the lungs, liver, and spleen and rapid

clearance by the RES. In extreme cases, this can lead to rapid blockage of pulmonary capillaries and acute mortality in animal models. Therefore, cationic polymers are typically synthesized as diblock copolymers with hydrophilic polymers such as PEG and used to form PIC micelles.[6] Kataoka's group pioneered the development of these micelles and their application as gene vectors. They used PEG-b-poly(Lysine) (PEG-PLA) as a diblock copolymer to condense DNAs and form PIC micelles that utilize PEGylation to shield their cationic component. Though PLys has a high pKa that limits its proton sponge and endosomal escape capacity, this approach has served as the basis for numerous subsequent designs that utilize polyion complex formation to produce stable, nucleic acid-loaded micelles.

Micelle surface functionalization with targeting moieties can be beneficial for both PEGylated and non-PEGylated micelles. Stayton et al. employed this approach to their cationic micelles by conjugating folate for cancer cell targeting.[7] They were able to exhibit folate receptor specific interaction of the folate conjugated micelles as well as in vitro gene knockdown, though this system is also not optimized for intravenous delivery due to high residual surface charge. More commonly, targeting moieties are added to the surface of PEGylated micelles. Kataoka et al. attached targeting molecules to their PEGylated PIC micelles for various applications.[8] They attached lactose for targeting the ASGP receptor of HepG2 cells, showing a significant increase in cellular transfection efficiency compared with micelles lacking lactose.[9] They also employed the cyclic RGD peptide as a means to target αvβ3 integrin receptors. This integrin is expressed on many cell types that play an important role in angiogenesis, and is a potentially useful means to target anti-angiogenic tumor therapies. In these studies, this targeting approach improved PIC micelle tumor delivery of pDNA encoding suicide genes.[10] Hydrophobic stabilization of the core in PIC micelles has also been employed in order to achieve better pharmacokinetics in vivo.[11] By

balancing cationic DMAEMA with hydrophobic BMA within the core of PEG-*b*-p(DMAEMA-*co*-BMA) polyplexes, significantly higher endosomal escape and luciferase protein level knockdown was achieved in vitro. As a result of the improved stability and pharmacokinetics of this carrier system, it was able to produce knockdown of the model gene PPIB in vivo without any active targeting moiety.

Chapter II

Combinatorial Library of Ternary Polyplexes Enables Identification of Improved siRNA Nanocarriers

Abstract

A new library of ternary siRNA polyplexes formed of combinatorially combined pH-responsive polymers was developed and screened for gene silencing efficacy in vitro and in vivo. [2-(dimethylamino)ethyl methacrylate] (DMAEMA)- and butyl methacrylate (BMA)-containing polymers were synthesized via reversible addition – fragmentation chain transfer (RAFT) polymerization. Ternary polyplexes were formed by varying the amounts and ratio of core-forming copolymers to corona-forming PEGylated, diblock copolymers during polyplex assembly. This library was developed such that structure-activity relationships of pH-responsive polymeric nanoparticles such as polyplex surface PEGylation density, size, stability, and endosomolysis could be systematically studied, and the relative importance of design parameters identified. The lead ternary polyplex formulation identified from multiparametric in vitro screening, DB-50B412, was optimally PEGylated with enough PEG to ensure colloidal stability (no change in size by DLS between 0 and 24 hr) and neutral surface charge (-1.86 mV) but had higher cell uptake (>90% positive cells) than the most densely PEGylated particles. The DB-50B412 polyplexes also incorporated the most hydrophobic and endosomolytic core-forming polymer, resulting in robust endosomolysis and in vitro siRNA silencing (~85% protein level knockdown) of the model gene luciferase. The potential efficacy of our lead ternary polyplex was further validated in vivo and benchmarked against binary polyplexes of the corona-forming PEGylated diblock. The DB-50B412 polyplex exhibited a reduced level of renal clearance after intravenous administration,

resulting in enhanced pharmacokinetics (1.6-fold increased area under the curve (AUC)) and consequently increased enhanced permeation and retention (EPR)-driven tumor accumulation (2.6-fold higher) compared to binary polyplexes. The combined cell- and systemic-level delivery benefits achieved with DB-50B412 resulted in significantly better in vivo gene silencing in an orthotopic mammary tumor model after both intratumoral (54% protein level knockdown, 1 injection) and intravenous (54% protein level knockdown, 3 injections) administration.

Introduction

RNA interference (RNAi) was initially observed by Mello and Fire et al. in 1998[12], and soon thereafter siRNAs were confirmed as short double-stranded nucleic acid molecules capable of potent and highly specific inhibition by RNAi.[13, 14] Currently, cellular and systemic delivery barriers limit the applications of siRNA.[15] Naked siRNAs do not readily enter cells, have no inherent mechanism for endosome escape, and are rapidly cleared through filtration in the kidneys after systemic administration.[16, 17] Thus, the use of siRNA as a safe and efficacious therapeutic is contingent upon its effective delivery to the desired tissue, cell type, and sub-cellular compartment of interest. To date, a variety of methodologies have been developed to overcome the challenge of siRNA delivery, including covalent modifications[18, 19], antibody-protamine fusion[20], liposomal encapsulation[21], and nanoparticle formulations of cationic lipids or polymers.[22-24]

Packaging of siRNA by cationic nanoparticle formulations is one of the most investigated approaches.[25, 26] By this approach, siRNA is packaged onto nanocarriers with a large excess of cationic charge which serves to drive cellular uptake through interaction with the anionic cellular membrane.[27] Moreover, surface PEGylation has been widely employed as a strategy to neautralize these carriers for reduced opsonization and increased stealth from the mononuclear phagocyte

system (MPS) for systemic administration in vivo.[28-30] However, merely cationic polyplexes, PEGylated for systemic administration, still suffer from a lack of stability in vivo. This class of polyplexes, formed by electrostatic interaction, are disassembled at the glomerular basement membrane (GBM) and cleared primarily through the kidneys, resulting in modest increases of circulation time over naked siRNA.[31, 32] In previous work, we endeavored to improve the performance of cationic polyplexes through the incorporation of hydrophobicity into the core of the polyplex.[11] This approach led to polyplexes with enhanced intracellular delivery of siRNA and improved in vivo bioactivity in the liver, kidneys, and spleen.

Efforts to develop effective siRNA transfection reagents by combinatorial approaches have been successful, yielding potent reagents that rival viral constructs. Green, Langer, Anderson, et al. have developed large libraries of poly(β-amino esters) (PBAEs) and lipid or lipid-like nanoparticles through combinatorial methods with great success. Green et al. initially developed a library of cationic PBAEs in which the lead reagents were able to achieve pDNA transfection comparable to adenoviruses[33] and have more recently developed libraries which yielded PBAE derivatives highly effective at delivering siRNA and pDNA to glioblastomas.[34, 35] Anderson and Langer have used combinatorial synthesis methods to develop large libraries of cationic lipid and lipid-like nanoparticles, reporting the most potent in vivo siRNA knockdown in multiple animal models to date.[22, 36, 37]

In this work, we expand upon previous findings showing the importance of hydrophobic stabilization of cationic polyplexes and use a combinatorial approach to systematically study important structure-function relationships of PEGylated siRNA polyplexes and yield a potent in vivo siRNA delivery reagent. Moreover, a multiparametric in vitro screening methodology was employed in order to optimize siRNA polyplexes for simultaneously overcoming cell-level

barriers (uptake/endosomal escape) and systemic barriers (stability for long circulation and reduced renal clearance) following intravenous administration.

Poly(2-(dimethylamino)ethyl methacrylate) (pDMAEMA, DM), poly[(2-(dimethylamino)ethyl methacrylate)-*co*-(butyl methacrylate)] (p(DMAEMA-*co*-BMA), DB), poly[(ethylene glycol)-*b*-(2-(dimethylamino)ethyl methacrylate)] (PEG-*b*-p(DMAEMA), 0B), and poly[(ethylene glycol)-*b*-[(2-(dimethylamino)ethyl methacrylate)-*co*-(butyl methacrylate)]] (PEG-*b*-p(DMAEMA-*co*-BMA), 50B) were synthesized via RAFT polymerization. Ternary polyplexes were formed at varying N:P ratios (ratio of polymer amines:nucleic acid phosphates) and varying ratios of the core (DM/DB) to corona forming polymers (0B/50B) for three classes of formulations: DB core/0B corona [DB-0B], DB core/50B corona [DB-50B], and DM core/50B corona [DM-50B] to produce a library. This strategy affords surface charge neutral, siRNA core-loaded polyplexes stabilized by electrostatic and hydrophobic interactions with the ability to rapidly tune the polyplex core-corona composition and degree of surface PEGylation. Through this ternary complex/combinatorial approach, we were able to systematically study important polyplex characteristics such as surface PEGylation density, size, stability, and endosomolysis. Ternary polyplexes which were optimized to overcome multiple barriers to siRNA delivery achieved the highest gene silencing and incorporation of the DB core was identified as a crucial parameter for achieving siRNA silencing in vitro. The lead ternary polyplex identified from multiparametric screens was validated in vivo, showing favorable pharmacokinetics, biodistribution, and efficiently accumulating in and achieving gene specific siRNA silencing in an orthotopic mammary tumor model.

Materials and Methods

2.1 Materials. All chemicals were purchased from Sigma-Aldrich (St. Louis, MO, USA) unless otherwise specified. DMAEMA and BMA monomers were passed twice through a basic alumina gravity column prior to use in order to remove inhibitors. 2,2-Azobis(2-methylpropionitrile) (AIBN) was recrystallized twice from methanol. All cell culture reagents were purchased through Fischer Scientific unless otherwise specified. Cell culture media and reagents, including Dulbecco's Modified Eagle Medium (DMEM), Fetal Bovine Serum (FBS), PBS (-/-), PBS (+/+), and gentamycin were purchased through Life Technologies (Grand Island, NY, USA).

2.2 Synthesis of 4-Cyano-4-(ethylsulfanylthiocarbonyl)sulfanylpentanoic acid (ECT) and PEG-ECT macro-Chain Transfer Agent (macro-CTA). ECT, the RAFT CTA, was synthesized according to a previously reported procedure.[38] The terminal carboxylic acid of ECT was then conjugated to PEG.[11] Briefly, methoxy-PEG (2 mmol, 10 g, Mn = 5000 Da), ECT (4 mmol, 1.045 g), and Dimethylaminopyridine (DMAP, 0.08 mmol, 10 mg) were dissolved in dry DCM (50 mL) and dicyclohexylcarbodiimide (DCC, 4 mmol, 0.82 g) was added while stirring. The reaction mixture was stirred for 48 h at RT. Precipitated cyclohexyl urea was removed by filtration. DCM layer was concentrated and precipitated into diethyl ether twice. The precipitated PEG-ECT was washed thrice with diethyl ether and dried under vacuum. ^{1}H NMR (400 MHz Sprectrometer, Brüker, $CDCl_3$) showed 84% ECT conjugation to PEG.

2.3 Polymer Synthesis and Characterization. RAFT polymerization was used to synthesize all four polymers, either from ECT or the PEG-ECT macro-CTA. DMAEMA-*co*-BMA (DB) and pDMAEMA (DM) were synthesized from ECT (Figure 2a). In both cases, the target degree of polymerization was 150, reaction volume was 3 mL (Dioxane), degassing was done for 30 min by

nitrogen purge, and the polymerizations proceeded at 70 °C for 20 h using AIBN as an initiator at 10:1 (CTA:AIBN) molar ratio. Reactions were stopped by removing the flask from heat and opening the reaction to air. The reaction mixtures were transferred to dialysis tubing and dialyzed one day against methanol and one day more against diH_2O to remove unreacted monomers and ECT prior to lyophilization. PEG-*b*-pDMAEMA (0B) and PEG-*b*-p(DMAEMA-*co*-BMA) (50B) were synthesized from the PEG-ECT macro-CTA (Figure 2a). The target degrees of polymerization were 100 and 150, respectively. Reaction volumes were 3 mL (Dioxane), degassing was done for 30 min by nitrogen purge, the polymerizations proceeded at 70 °C for 20 h, and AIBN was used as an initiator at 10:1 (macro-CTA:AIBN) molar ratio. Reactions were stopped by removing the flask from heat and opening the reaction to air. The resulting diblock copolymers were precipitated in a cold solution of pentane:diethyl ether (90:10). The isolated polymers were dried, re-dissolved in ethanol, dialyzed one day against diH_2O and lyophilized to yield the final product. Polymers were characterized for composition and molecular weight (Mn) by ^{1}H NMR (400 MHz Sprectrometer, Brüker, $CDCl_3$). Absolute molecular weight and polydispersity (PI) were further determined by gel permeation chromatography (GPC) using DMF + 0.1 M LiBr as the mobile phase with inline Agilent refractive index and Wyatt miniDAWN TREOS light scattering detectors. Serial dilutions (10 mg/ml – 0.25 mg/ml) in DMF were measured on a digital refractometer to determine dn/dc values for calculating absolute molecular weight on GPC.

2.4 Assembly of siRNA loaded ternary polyplexes and size, zeta potential, and stability characterization. Three combinations of polymers were utilized for forming ternary polyplexes: DB-0B, DB-50B, and DM-50B. All polymers were dissolved in pH 4.0 citric acid buffer (10 mM).

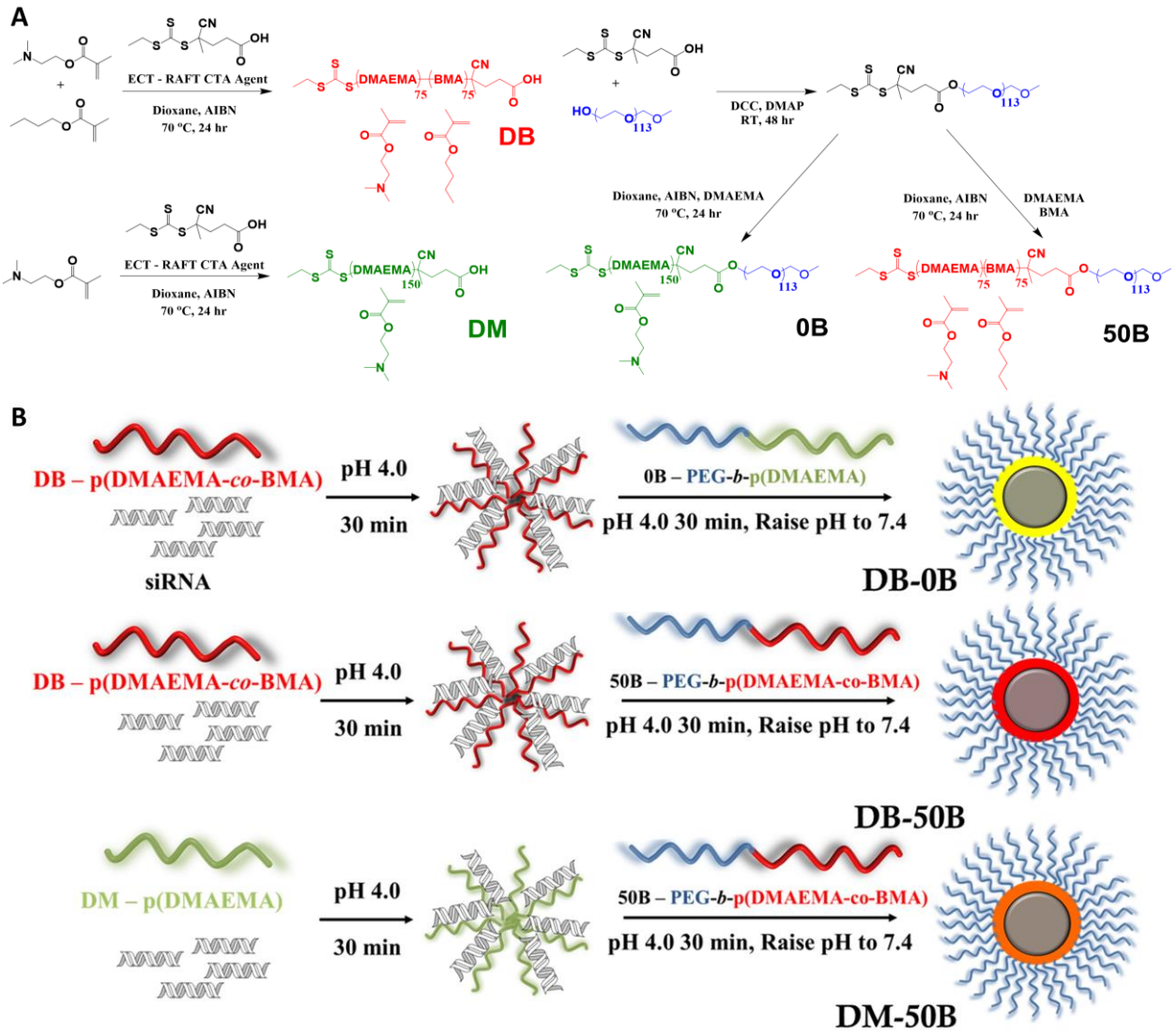

Figure 2. Polymer synthesis and ternary polyplex formation. (A) Four single-pot reactions yield the DB, DM, 0B, and 50B polymer units for forming unique classes of ternary polyplexes. (B) Three major classes of ternary polyplexes (DB-0B, DB-50B, and DM-50B) formed in aqueous milieu by complexing with siRNA at pH 4.0 and subsequently raising the pH to drive polyplex assembly.

siRNA was pre-condensed with the binary, core-forming polymer at each specified N:P ratio for 30 min at 1 mg/ml polymer concentration. Next, differing amounts of ternary, corona-forming polymer were added in order to give the appropriate final N:P ratio and let complex for an additional 30 min. Polymer amounts needed to yield final N:P ratios were determined according to the following two equations for binary (1) and ternary (2) polyplexes:

(1) $$nmol\ Pol = \frac{(nmol\ NA)(bp\ NA)(2)(N{:}P)}{(RU\ DMAEMA)(0.5)}$$

(2) $$nmol\ Pol2 = \frac{(nmol\ NA)(bp\ NA)(2)(N{:}P) - (nmol\ Pol1)(RU\ DMAEMA1)(0.5)}{(RU\ DMAEMA2)(0.5)}$$

where nmol Pol is the nmol of binary polymer, nmol NA is the nmol of nucleic acid, N:P is the ratio of primary amines to phosphates, RU DMAEMA is the number of repeating units of DMAEMA within the polymer backbone, nmol Pol2 is the nmol of ternary, corona-forming polymer, nmol Pol1 is the nmol of binary, core-forming polymer, RU DMAEMA1 is the repeating units of DMAEMA within the binary, core-forming polymer backbone, and RU DMAEMA2 is the repeating units of DMAEMA within the ternary, corona-forming polymer. A 5-fold excess of pH 8.0 phosphate buffer (10 mM) was added to every sample before filtering through 0.45 μm pore syringe filters and measuring hydrodynamic diameter (D_h) and zeta potential (ζ) of the resulting ternary polyplexes at 0 and 24 h using dynamic light scattering (DLS) (Malvern Zetasizer Nano ZS, Malvern, UK). The naming scheme used for ternary polyplex formulations is as follows: [Binary Polymer]-[Ternary Polymer](Binary N:P)(Ternary N:P). For example, the lead ternary polyplex which contains a DB core formulated at 4:1 N:P and 50B corona formulated to a final N:P of 12:1 reads as DB-50B412.

2.5 Characterization of pH-dependent membrane disruption by the hemolysis assay. The hemolysis assay was used to assess the potential for all ternary polyplex formulations to escape the endolysosomal pathway. Red blood cells (RBCs) were obtained from anonymous donors and isolated by a previously reported and well-established protocol.[39] After isolation, RBCs were incubated with varying concentrations (5, 15, and 30 μg/ml) of each ternary polyplex formulation at four pH's indicative of extracellular and endolysosomal ranges (7.4, 6.8, 6.2, 5.6). After 1 h of incubation, intact RBCs and any debris were centrifuged out, and supernatants were removed. The

supernatants were measured for absorbance at 451 nm (hemoglobin absorbance) and percent hemolysis was determined relative to 1% Triton-X100 detergent.

2.6 Cell Culture. Human epithelial breast cancer cells (MDA-MB-231) and mouse embryonic fibroblasts (NIH3T3) were cultured in DMEM supplemented with 10% FBS and 50 μg/mL gentamicin. MDA-MB-231 and NIH3T3 cells were transfected with Lentiviral Expression particles for firefly luciferase, Green Fluorescent Protein (GFP), and Blasticidin resistance resulting in the generation of luciferase expressing-MDA-MB-231 (L231) and NIH3T3 (L3T3) cell lines.

2.7 Cytocompatability of ternary polyplexes. Cytocompatability of all formulations of ternary polyplexes was evaluated by adding scrambled siRNA containing ternary polyplexes to L231 and L3T3 cells and measuring relative cell number based on cellular luminescence. All polymers were dissolved in pH 4.0 citrate buffers (10 mM, 3.33 mg/ml) and binary, core-forming polymers were incubated with a siRNA for 30 min at the appropriate N:P ratio determined by equation (1) above. Next, the ternary, corona-forming polymer (10 mM, pH 4.0 citrate, 3.33 mg/ml) was added in order to yield the appropriate final N:P ratio determined by equation (2) above and incubated for 30 min. A 5-fold excess of pH 8.0 phosphate buffer (10 mM) was then used to raise the solutions to pH 7.4. L231 and L3T3 cells were seeded to 96-well black-walled plates at a density of 2,000 cells/well and allowed to adhere overnight. Ternary polyplex formulations were then added to each well in full serum media (DMEM, 10% FBS, 50 μg/mL gentamicin) at a final siRNA concentration of 100 nM and incubated with the cells for 24 h. After 24 h, media was replaced with luciferin containing media (150 μg/ml) and luminescence signal was collected on a Lumina III IVIS system (Xenogen Corporation, Alameda, CA, USA).

2.8 Cell uptake of ternary polyplexes. Cell uptake was evaluated in both MDA-MB-231 and NIH3T3 cell types by flow cytometry. MDA-MB-231 and NIH3T3 cells were seeded to 24-well plates at a density of 30,000 cells/well and allowed to adhere overnight. Ternary polyplexes were prepared by the same procedure above, substituting alexa488-labeled dsDNA for siRNA. Alexa488-dsDNA loaded ternary polyplexes were added to each well to give a final dsDNA concentration of 100 nM and incubated with cells in full serum media (DMEM, 10% FBS, 50 μg/mL gentamicin) for 24 h. After 24 h, media with treatments was removed, cells were washed with PBS (-/-), trypsinized (0.25%), transferred to microcentrifuge tubes, and centrifuged at 420g for 7 min to yield a stable pellet of cells. Pellets were re-suspended in 0.4 mL PBS(-/-) with 0.04% trypan blue to quench extracellular fluorescence and monitored by FACS (FACSCalibur, BD Biosciences, Franklin Lakes, NJ, USA) at excitation wavelength of 488 nm and emission wavelength of 519 nm to quantify intracellular delivery of dsDNA.

2.9 In vitro siRNA silencing by ternary polyplexes. The gene silencing profile of ternary polyplex formulations was screened within L3T3 fibroblasts. L3T3s were initially seeded in black-walled, 96-well plates at a density of 2,000 cells/well and allowed to adhere overnight. Cells were then treated for 24 h in full-serum media (DMEM, 10% FBS, 50 μg/mL gentamicin) with all ternary polyplex formulations prepared as described above and containing an anti-luciferase siRNA sequence (100 nM). After 24 h, treatment media was replaced by luciferin containing media (150 μg/ml) and cellular luminescence was measured using an IVIS Lumina III imaging system (Xenogen Corporation, Alameda, CA, USA). The cells were then incubated for an additional 24 h after luciferin containing media was replaced by low-serum media (DMEM, 1% FBS, 50 μg/mL gentamicin). Cellular luminescence was re-measured at 48 h and normalized to a scrambled control siRNA sequence in all cases.

2.10 Ternary polyplex biodistribution and blood pharmacokinetics. *Biodistribution in CD-1 mice*. Fluorescent polyplexes were formed as described above, with 0.1 mg/mL solution of binary polymer, by complexing with Cy5-labeled dsDNA at the optimal ternary N:P ratio (4:1/12:1 Binary/Ternary) determined by in vitro screening. CD-1 mice (4-6 weeks old, Charles Rivers Laboratories, Wilmington, MA, USA) were injected via the tail vein with 1 mg/kg (dsDNA dose) of fluorescent polyplexes. After 20 min, animals were sacrificed and the organs of interest (heart, lungs, liver, spleen, and kidneys) were excised. The organs were fluorescently imaged and quantified on an IVIS Lumina III imaging system (Xenogen Corporation, Alameda, CA, USA) at excitation wavelength of 620 ± 5 nm and emission wavelength of 670 ± 5 nm (n = 6).

Blood plasma pharmacokinetics. Blood was collected retro-orbitally at 5 min and 10 min post-injection, not exceeding two collections per animal. After 20 min, animals were sacrificed, and blood was immediately collected via the renal vein. Blood samples were centrifuged at 2000 x g for 5 min and 5 μL of plasma was taken from the supernatant and diluted into 95 μL PBS (-/-). Fluorescence was measured and quantified on an IVIS Lumina III imaging system (Xenogen Corporation, Alameda, CA, USA) at excitation wavelength of 620 ± 5 nm and emission wavelength of 670 ± 5 nm (n = 6). A standard curve was generated by measuring the fluorescence of the initial fluorescent polyplex solution in PBS (-/-) over the range of 200% - 1.5% of the injected dose. The standard curve was utilized in order to calculate the percent of injected dose in each blood sample, and the calculated values were used to determine siRNA concentration in the plasma at each time point as well as area under the curve (AUC) values.

Biodistribution in athymic nude tumor-bearing mice. Athymic nude female mice (4-6 weeks old, Jackson Laboratory, Bar Harbor, ME, USA) were injected in each mammary fat pad with 1 x 10^6 L231 cells in DMEM:Matrigel (50:50). After 17 days, tumor-bearing mice were

injected via the tail vein with 1 mg/kg (dsDNA dose) of fluorescent polyplexes. After 20 min, animals were sacrificed and the organs of interest (heart, lungs, liver, spleen, kidneys, and tumors) were excised. The organs were fluorescently imaged and quantified on an IVIS Lumina III imaging system (Xenogen Corporation, Alameda, CA, USA) at excitation wavelength of 620 ± 5 nm and emission wavelength of 670 ± 5 nm (n = 6).

2.11 In vivo siRNA silencing by ternary polyplexes. *Intratumoral (i.t.) siRNA silencing.* Athymic nude female mice (4-6 weeks old, Jackson Laboratory, Bar Harbor, ME, USA) were injected in each mammary fat pad with 1 x 10^6 L231 cells in DMEM:Matrigel (50:50). After 17 days, tumor-bearing mice were injected intraperitoneally (i.p.) with luciferin substrate (150 mg/kg) and imaged for bioluminescence on an IVIS Lumina III imaging system (Xenogen Corporation, Alameda, CA, USA) 20 minutes post-injection. Next, the mice were injected i.t. with 1 mg/kg (siRNA dose) polyplexes containing either anti-luciferase siRNA, a scrambled control siRNA, or saline. After 24 hours, the mice were re-injected with luciferin (150 mg/kg) and imaged for bioluminescence 20 min post-injection of luciferin. For quantification, the ratio of bioluminescence of anti-luciferase siRNA treated to scrambled siRNA treated tumors was determined within each mouse and the percent luciferase activity was calculated as: ratio at 24 hr/ratio at 0 hr (n = 5).

Intravenous (i.v.) siRNA silencing. Athymic nude female mice (4-6 weeks old, Jackson Laboratory, Bar Harbor, ME, USA) were injected in each mammary fat pad with 1 x 10^6 L231 cells in DMEM:Matrigel (50:50). After 17 days, tumor-bearing mice were injected i.p. with luciferin substrate (150 mg/kg) and imaged for bioluminescence on an IVIS Lumina III imaging system (Xenogen Corporation, Alameda, CA, USA) 20 minutes post-injection. Next, the mice were injected via the tail vein with 1 mg/kg (siRNA dose) polyplexes containing either anti-

luciferase siRNA, a scrambled control siRNA, or saline. Mice were imaged and dosed at days 17, 18, and 19 and imaged again on days 20 and 24. Relative luminescence was determined by measuring the raw luminescent intensity of each tumor on each day and comparing to the initial signal at day 17 (n = 6).

Results and Discussion

3.1 Polymer Synthesis and Characterization. The two core-forming, binary copolymers (DB and DM) and two shell-forming, ternary diblock copolymers (0B and 50B) were synthesized from either the RAFT CTA ECT or 5 kDa macro-CTA PEG-ECT, respectively (Figure 2a). RAFT polymerization is advantageous for the synthesis of biomacromolecules which require complex architectures with precise and monodisperse products.[40, 41] All four polymers were synthesized with low polydispersity indices (M_w/M_n < 1.3) and resulted in products close to the targeted composition and molecular weight (Figures S2 and S3). Moreover, the simple and single-step polymerizations used herein are scalable and yield polymers which can be rapidly purified. These polymers were chosen as the base units of three distinct classes of core-shell ternary polyplexes (DB-0B, DB-50B, and DM-50B) which build on previous work showing that balancing cationic siRNA polyplexes with hydrophobicity can help overcome cell-level and systemic siRNA delivery barriers that limit the effectiveness of strictly cationic polyplexes.[11, 42-44] Within each class, the amount of core-forming binary polymer, shell-forming ternary polymer, and the ratio of the two were varied in order to systematically study the effects of each component as well as investigate structure-function relationships such as surface PEGylation density, size, stability, endosomolysis, and composition of the resulting polyplexes in vitro and in vivo.

3.2 Physicochemical characterization of siRNA-loaded polyplexes. Polyplex size, surface zeta potential, and stability are crucial parameters when designing a systemic delivery system for siRNA.[25] Optimal polyplexes have small size (20 – 50 nm) for enhanced tissue penetration[45], neutral zeta potential for avoiding aggregation with serum proteins, opsonization, and detection and clearance by the MPS[42, 46], and are colloidally stable for circulation in the blood plasma.[47] Thirty ternary polyplexes were formed from varying N:P ratios and varying ratios of the core- to corona-forming polymers within each class of ternary polyplex (DB-0B, DB-50B, and DM-50B) in order to generate a combinatorial library (Figure 2b). The library was initially screened for size at 0 h and 24 h and zeta potential by DLS to indicate which polyplexes were physicochemically optimal for systemic administration. DB-0B, DB-50B, and DM-50B ternary polyplexes all formed stable and significantly more compact polyplexes (~15 – 40 nm) than the 0B or 50B (~100 nm) binary polyplexes (Figure 3). Additionally, polyplex stability at 24 h was directly related to amount of corona-forming polymer and consequently the degree of surface PEGylation (Figures 3 and S4). As the degree of PEGylation was increased, a threshold was reached in each class where aggregation was prevented at 24 h and further PEGylation above the threshold showed no added benefit. The zeta potential for all polyplexes screened was between +5 and -5 mV, which is optimal for systemic administration. In sum, the initial physicochemical screening of this library of ternary polyplexes identified a subgroup of promising formulations with advantageous characteristics for effective siRNA delivery in vivo.

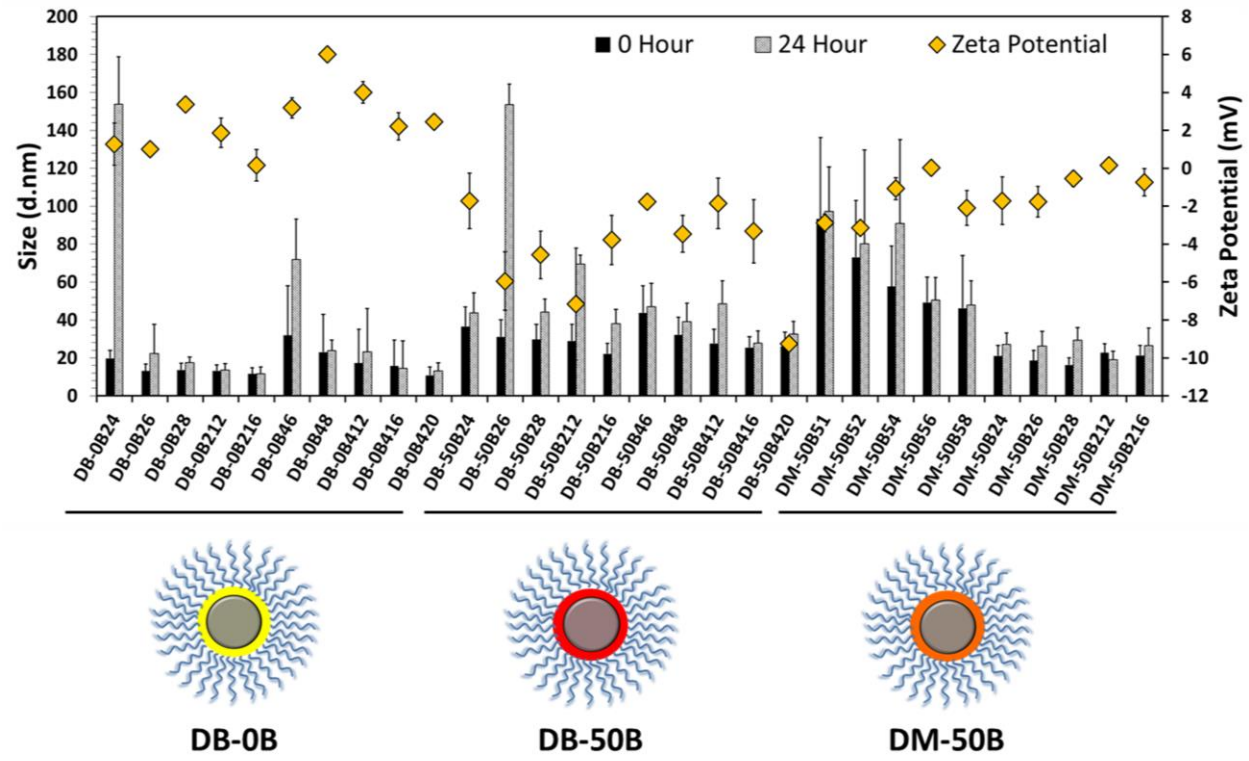

Figure 3. Size and zeta potential of library of ternary polyplexes consisting of all three classes of polyplexes at varying ratios of core- to corona-forming polymer.

3.3 Characterization of pH-dependent membrane disruption. Entrapment in the endolysosomal pathway and subsequent degradation or trafficking out of the cell limit the effectiveness of many biologic drugs including siRNA.[48, 49] The hemolysis assay was used as an initial indicator of the potential for ternary polyplexes to escape the endolysosomal pathway and deliver siRNA to the site of activity within the cytosol. Hemolysis was exhibited by all classes of ternary polyplexes investigated. However, ternary polyplexes which had 50B in the corona had more desirable hemolysis profiles than 0B corona polyplexes. The 50B-containing polyplexes showed switch-like endosomolytic behavior at the early endosomal pH 6.8, whereas 0B-containing polyplexes had weak hemolysis and exhibited hemolysis at the extracellular/physiological pH 7.4 (Figure 4). The degree of hemolysis observed was also dependent upon the corona-forming

polymer. For the 0B corona, the degree of hemolysis decreased with increasing amounts of 0B polymer, indicating that the 0B polymer shielded the hemolytic DB core in a dose-dependent manner (Figure 4a). On the other hand, the degree of hemolysis was increased by adding increasing amounts of the 50B corona polymer (Figure 4b, c). This trend can be noticed by the hemolytic behavior at pH 6.8, which consistently increases as polyplexes contain more 50B corona-forming polymer. Therefore, ternary polyplexes which contained 50B as the corona-forming polymer exhibited optimal pH-dependent membrane disruptive behavior while 0B-corona ternary polyplexes exhibited sporadic hemolysis and in some cases showed hemolysis at pH 7.4, which we generally correlate with cytotoxicity.

3.4 In vitro cytocompatibility and cellular uptake of ternary polyplexes. The cytocompatibility and relative cell uptake of all ternary polyplexes were initially screened in L3T3 and NIH3T3 cells, respectively. The L3T3s, NIH3T3s which were made to constitutively express luciferase protein, offered the ability to quantify luminescence as a measure of cell number for determining cytocompatability. After 24 hours of incubation with polyplexes containing a scrambled control siRNA sequence, only the DB-0B class of polyplexes exhibited significant cytotoxicity compared to no treatment (Figure 5). The observed toxicity increased consistently as the amount of polymer was increased, and the polyplexes with the most DB core polymer (DB-0B46 – 420) approached 100% toxicity (Figure 5a). This result correlates with the observation of membrane disruption at pH 7.4 for some formulations as indicated from the hemolysis assay. No DB-50B or DM-50B polyplexes were significantly toxic compared to no treatment (Figure 5b, c), again correlating well with the observation of controlled, switch-like membrane disruption at the early endosomal pH 6.8 from the hemolysis assay.

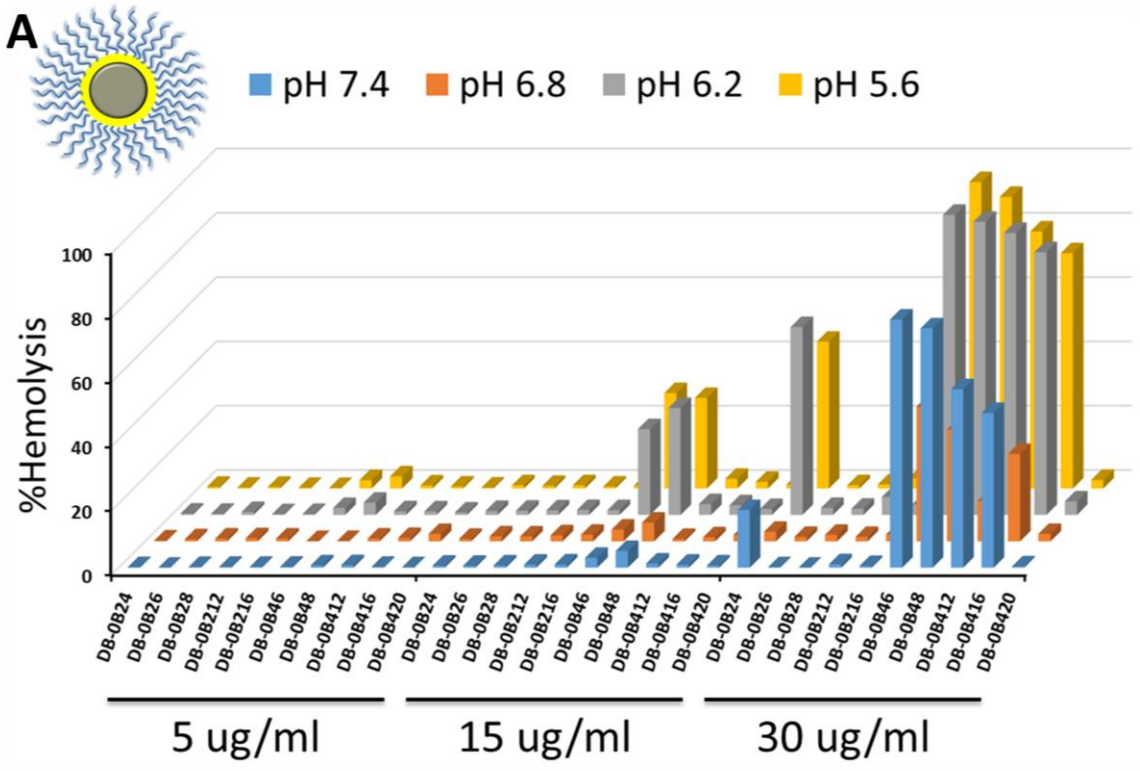
A
pH 7.4
pH 6.8
pH 6.2
pH 5.6
%Hemolysis
100
80
60
40
20
0
DB-0B24
DB-0B26
DB-0B28
DB-08212
DB-08216
DB-0B46
DB-0B48
DB-08412
DB-08416
DB-08420
5 ug/ml
15 ug/ml
30 ug/ml

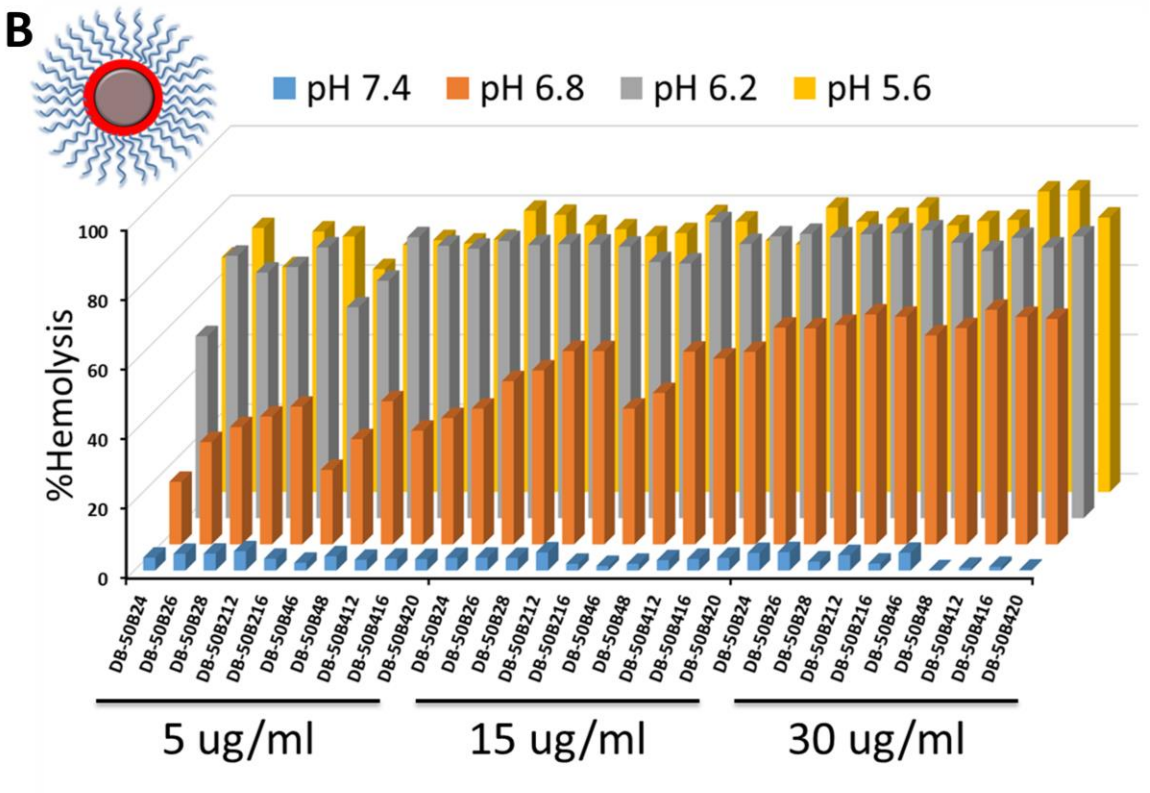
B
pH 7.4
pH 6.8
pH 6.2
pH 5.6
%Hemolysis
100
80
60
40
20
0
DB-50B24
DB-50B26
DB-50B28
DB-508212
DB-508216
DB-50B46
DB-50B48
DB-508412
DB-508416
DB-508420
5 ug/ml
15 ug/ml
30 ug/ml

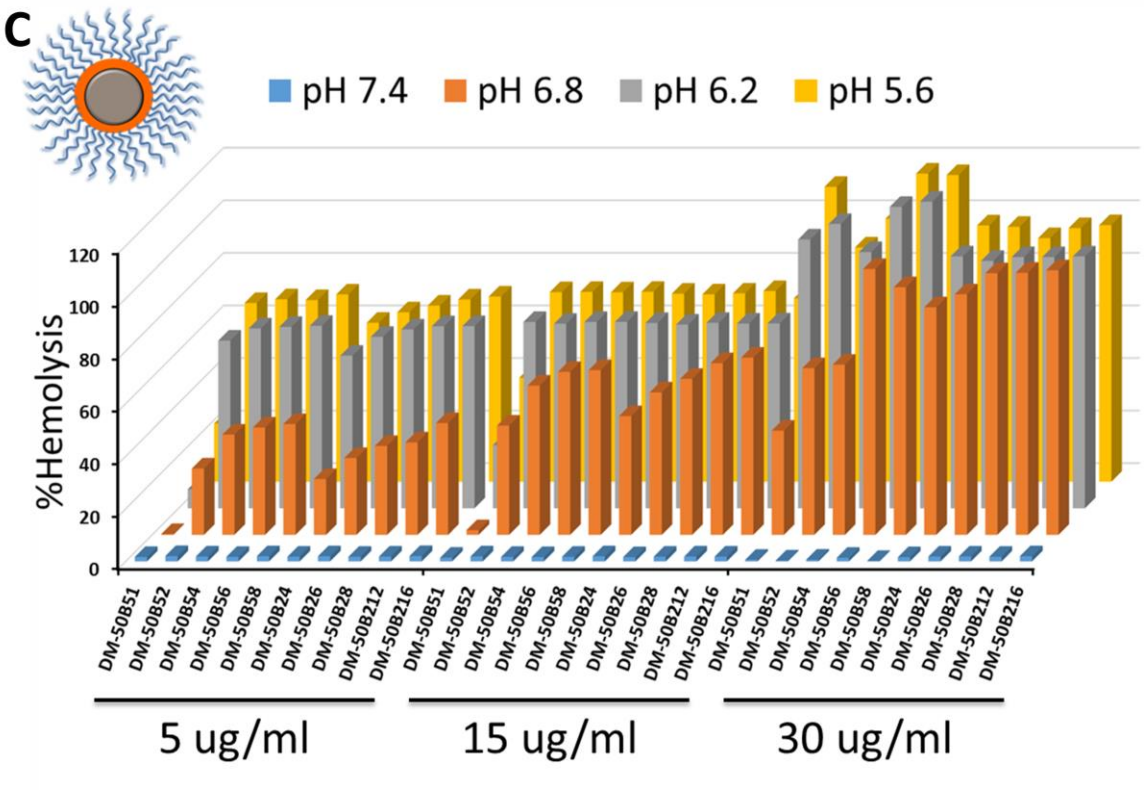

Figure 4. Hemolysis profiles of (A) DB-0B, (B) DB-50B, and (C) DM-50B ternary polyplexes.

Further, binary polyplex formulations of DB (DB2B and DB4B) approached 100% toxicity without the addition of a corona-forming ternary polymer (Figure 5a, b), suggesting that the corona-forming polymer effectively coats the DB core and that there is a significant cytocompatability benefit of polyplex PEGylation.

Cellular uptake was dependent upon the chemistry of the cationic block of the corona-forming ternary polymer as well as the ratio of the PEGylated, ternary and the core-forming, binary cationic polymers. DB-0B ternary polyplexes exhibited the highest cell uptake with up to 10-fold higher mean fluorescence intensity than DB-50B and DM-50B polyplexes (Figure 3d-f). However, DM-50B and DB-50B ternary polyplexes still exhibited up to 5-fold higher mean fluorescence intensity than their parent 50B binary polyplexes. The increasing fluorescence intensity observed

within the DM-50B51 – 58 polyplexes is due to incomplete complexing of the Alexa488-labeled dsDNA. The increasing intensity is observed as the polyplexes complex slightly more dsDNA for each increase in the final N:P ratio. In all other groups, a clear trend of decreasing cell uptake was observed for increasing degrees of PEGylation. After reaching an 8:1 final N:P ratio, each subsequent addition of more corona-forming PEGylated polymer significantly decreased cell uptake. Importantly, being able to control the amount of corona-forming polymer and thereby the density of PEGylation affords the ability to choose an optimal PEGylation state which provides colloidal stability and also a high level of cell uptake.

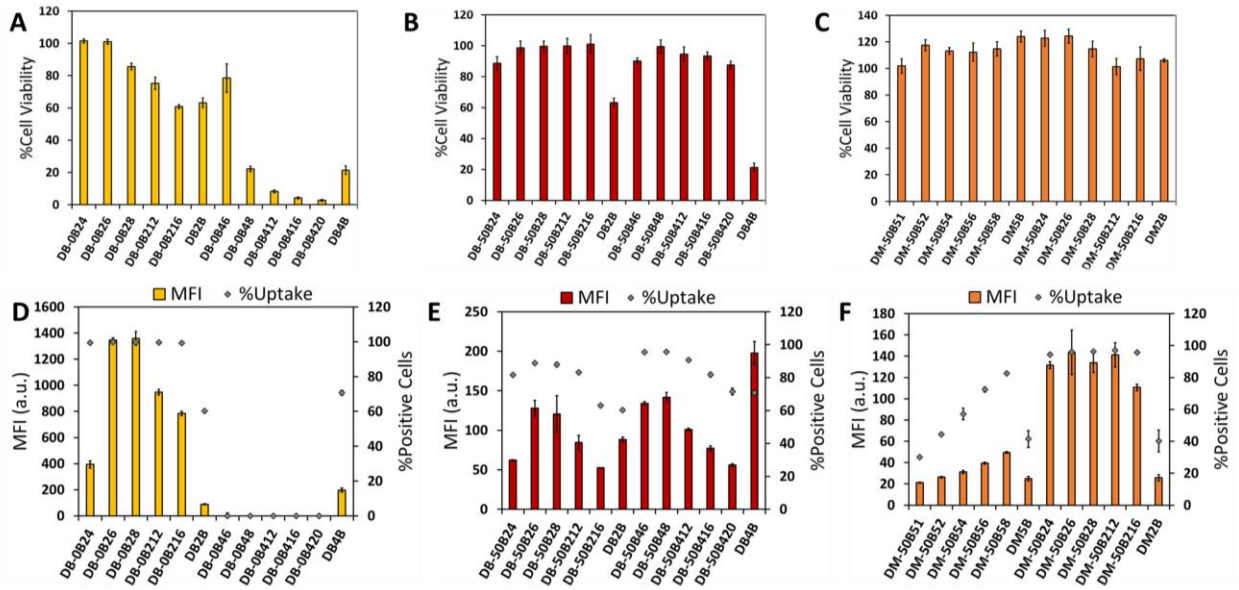

Figure 5. Ternary polyplex screens for cell viability and uptake in mouse embryonic fibroblasts (3T3s). Percent cell viability of (A) DB-0B, (B) DB-50B, and (C) DM-50B polyplexes. Cellular uptake of (D) DB-0B, (E) DB-50B, and (F) DM-50B polyplexes.

3.5 In vitro siRNA silencing by ternary polyplexes. The classes of ternary polyplexes were evaluated for in vitro target silencing of the model gene luciferase in L3T3 cells. Both DB-0B and DB-50B classes of ternary polyplexes achieved significantly greater siRNA knockdown (measured as protein level expression of luciferase at 48 h and normalized to scrambled siRNA control) than

their parent 0B and 50B binary polyplexes, respectively (Figure S6), as well as the best previously published ternary complexes.[50, 51] Although DB-0B polyplexes were taken up by cells up to 10-fold more than other polyplex classes, the DB-50B46 – 420 group of ternary polyplexes achieved the greatest knockdown with between 65 – 85% reductions in luciferase activity at 48 hr (Figure S6). Therefore, the DB-50B46 – 420 group of polyplexes may overcome other intracellular barriers (such as endosomal escape) more efficiently in order to account for their high knockdown despite their lower levels of cell uptake.

3.6 Multiparametric evaluation of combinatorial library of ternary polyplexes. The combinatorial library herein investigated was developed with the motivation that polyplexes which successfully overcome multiple siRNA delivery barriers will achieve the greatest in vitro gene silencing while also being most rapidly translatable to in vivo models of disease. Therefore, assays were chosen which directly address physiological barriers to siRNA delivery and which would indicate polyplex ability to overcome each of these barriers. Size and stability (size at 24 h) were measured by DLS for indicators of tissue penetration (size) and stability in the blood (stability) and cell viability was measured for indicating extracellular inertness and cytocompatibility. Flow cytometry was used to quantify polyplex cell internalization. Hemolysis, the amount of core-forming polymer, and whether the polyplex core contained DB were used to indicate endosomolytic capacity. Target gene silencing was used as a final readout to confirm the most effective polyplexes. As shown in Figure 6a, ternary polyplexes which perform best across multiple assays and which therefore overcome multiple delivery barriers achieve the greatest luciferase knockdown. Polyplex stability, cell uptake, and endosomolysis were further analyzed in order to determine the most important design parameters for achieving high siRNA knockdown. Stability was important for achieving knockdown, but it was not a perfect predictor as many

polyplexes which were stable did not achieve good knockdown and some polyplexes which were not stable did achieve knockdown (Figure 6b). In the same way, cell uptake was important for achieving knockdown, but many polyplexes which had close to 100% cell uptake did not achieve any knockdown. Finally, the presence of a DB core was one of the strongest indicators for achieving excellent gene knockdown. No polyplexes which did not contain the DB core achieved knockdown, whereas almost all polyplexes containing DB achieved knockdown. In sum, it was important to have polyplexes which were stable and had the highest uptake as prerequisites to achieving high knockdown, but the presence of the hydrophobic and endosomolytic DB core ensured a formulation which would effectively achieve gene knockdown. As a result of the multiparametric screen of our combinatorial library, the DB-50B46 – 420 class of polyplexes were identified as the most promising for in vivo translation. DB-50B412 was chosen as a lead candidate for in vivo testing because it possessed all good attributes of this class of polyplexes (stability, uptake, endosomolysis, and silencing) while using less material than DB-50B416 and DB-50B420 formulations.

3.7 Blood pharmacokinetics and biodistribution of lead ternary polyplexes. The lead ternary polyplex, DB-50B412, identified from multiparametric in vitro screening was tested in vivo in order to validate it as a potent siRNA nanocarrier for systemic delivery applications as well as validate that the multiparametric screening approach successfully resulted in a rapidly translatable reagent. The blood pharmacokinetics and biodistribution of DB-50B412 polyplexes were initially investigated in wild type CD-1 mice and benchmarked against the parent 50B binary polyplexes. Significantly higher amounts of fluorescence were detected in blood samples collected at each time point (5, 10 and 20 min) after tail vein injection of 1 mg/kg Cy5-dsDNA loaded polyplexes (Figure 7a).

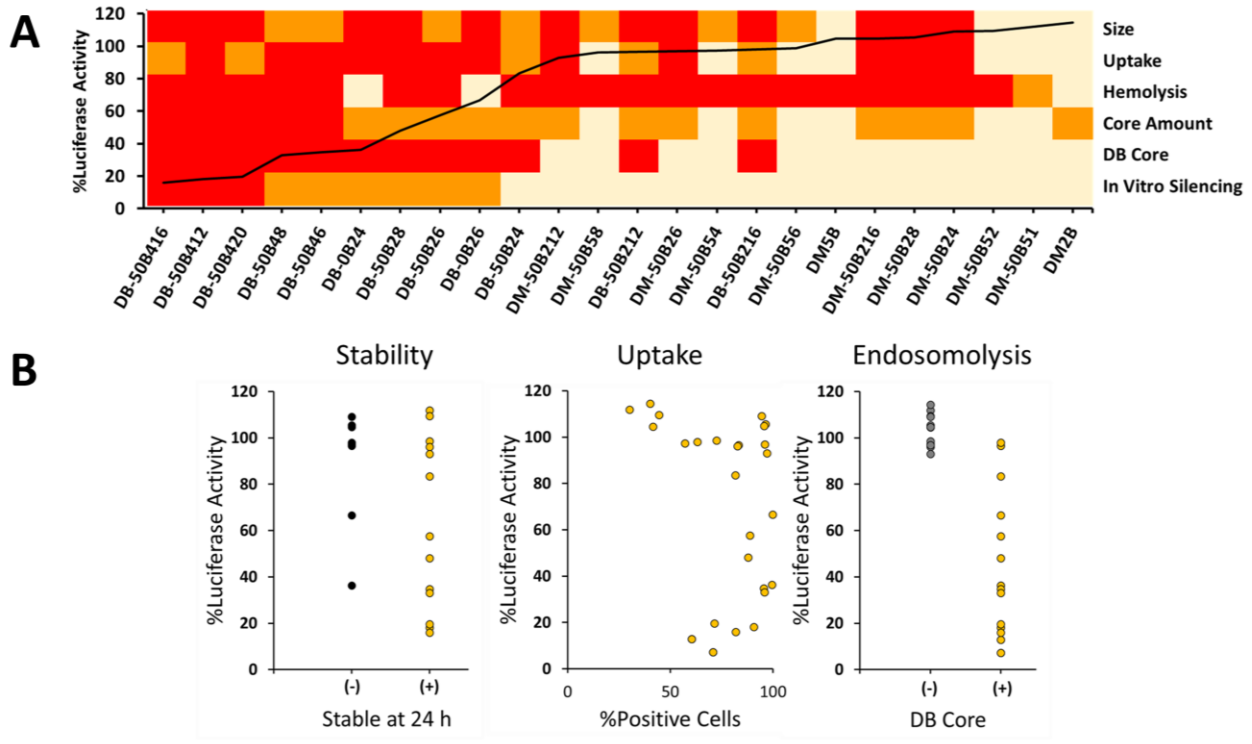

Figure 6. Multiparametric analysis of ternary polyplexes. (A) A heat-map representative of polyplex performance in multiple assays which predict the ability to overcome physiological barriers. (B) Measures of stability, uptake, and endosomolytic potential plotted against in vitro luciferase activity.

This led to a 1.6-fold increase in the area under the curve (AUC) value for DB-50B412 ternary polyplexes compared to 50B binary polyplexes. Passive tumor targeting is achieved by nanoparticles between ~20-200 nm through the enhanced permeation and retention (EPR) effect.[52] The amount of nanoparticles which are available to accumulate via the EPR effect is highly dependent upon the AUC of the nanoparticles, where nanoparticles which fall within the appropriate size range and have higher AUCs typically achieve more accumulation within tumors.[52, 53] Therefore, the increased AUC of DB-50B412 ternary polyplexes is important for improving siRNA delivery to tumors.

The biodistribution of DB-50B412 ternary polyplexes to major organs of interest and tumors was investigated in both wild type CD-1 mice and tumor-bearing athymic nude mice after

17 days of tumor growth (~75 – 150 mm^3). Consistent in both mouse models, the DB-50B412 ternary polyplexes exhibited significantly lower fluorescent signal in the kidneys (Figure 7b, c). Recent studies have identified the kidneys as the major route for clearance of siRNA polyplexes which are assembled by electrostatic interactions.[31, 32] In these studies, anionic proteoglycans such as heparin sulfate of the glomerular basement membrane were identified as the culprits for polyplex disassembly and subsequent rapid clearance through the kidneys. Therefore, it is important to reduce clearance through the kidneys as much as possible in order to achieve higher AUCs for i.v. administered siRNA polyplexes. In this case, DB-50B412 ternary polyplexes concomitantly exhibited a reduction in accumulation in the kidneys and increase in overall AUC when compared to their parent 50B binary polyplexes. Finally, DB-50B412 ternary polyplexes were detected at 2.6-fold higher levels in orthotopic tumors 20 min post-injection via the tail vein of 1 mg/kg Cy5-dsDNA loaded polyplexes (Figure 7c), consistent with the observed increase in AUC and principles of EPR-based tumor accumulation. In total, DB-50B412 polyplexes showed increased blood plasma AUC, reduced kidney accumulation, and increased tumor accumulation when compared to 50B binary polyplexes, all advantageous characteristics for effective systemic delivery of siRNA.

3.8 In vivo siRNA silencing by ternary polyplexes. The siRNA silencing efficacy of lead DB-50B412 ternary polyplexes was evaluated in vivo in athymic nude mice bearing orthotopic L231 tumors in the mammary fat pad. In order to directly assess local silencing efficacy, we began by looking at silencing after i.t. injections of 1 mg/kg anti-luciferase siRNA loaded polyplexes. After allowing tumors to grow for 17 days to a final volume of 75 – 150 mm^3, mice were injected i.t. in the right tumor with anti-luciferase siRNA loaded polyplexes and in the left tumor with scrambled siRNA loaded polyplexes as a contralateral control.

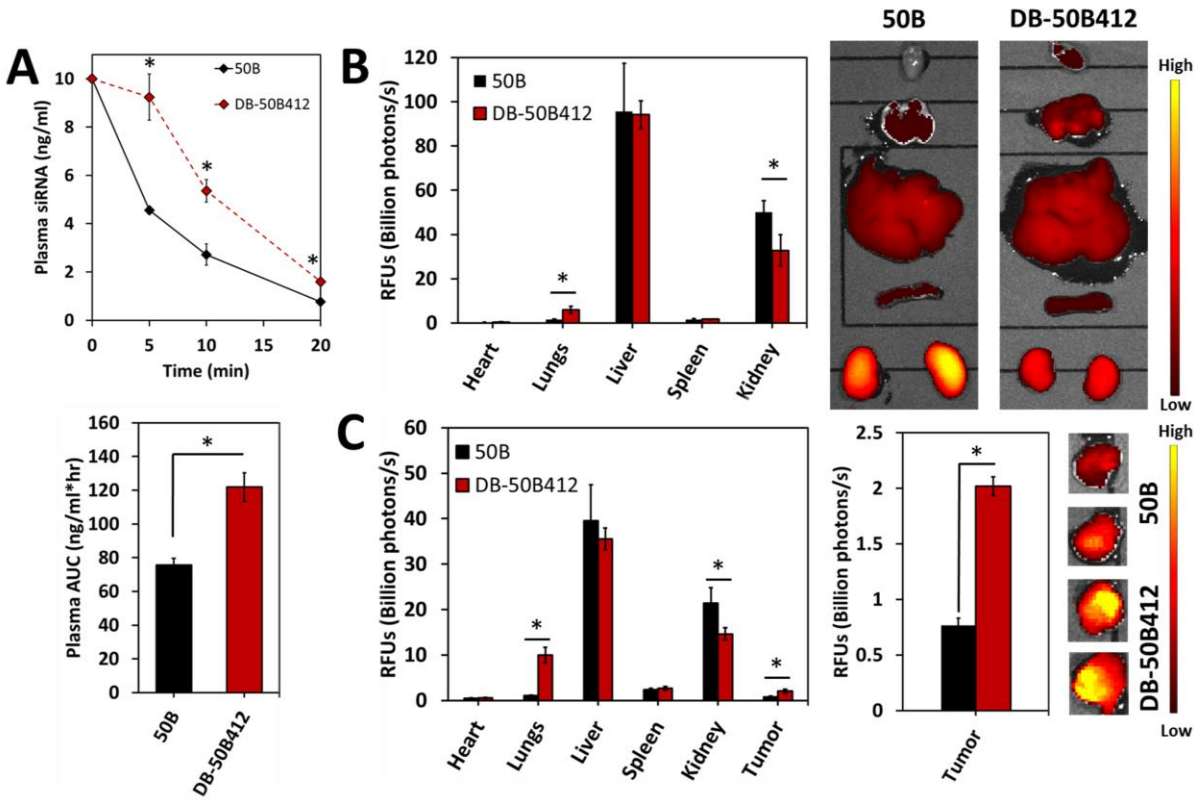

Figure 7. Blood pharmacokinetics and biodistribution of lead ternary polyplex. (A) Plasma concentration of siRNA and area under the curve (AUC) after tail vein injection of 1 mg/kg siRNA. (B) Ex vivo imaging and quantification of siRNA in major organs 20 min after tail vein injection of 1 mg/kg siRNA in CD-1 mice. (C) Ex vivo imaging and quantification of siRNA in major organs and tumors (2 per mouse) 20 min after tail vein injection of 1 mg/kg siRNA in tumor-bearing nude mice.

Another cohort was injected i.t. with saline as a no treatment control. 50B binary polyplexes achieved 28% silencing (compared to scrambled, $p = 0.62$) while DB-50B412 ternary polyplexes achieved 54% silencing (compared to scrambled, $p = 0.02$) 24 hr after a single i.t. injection (Figure 8a, b). The promising pharmacokinetics/biodistribution data along with achieving a significant local silencing effect motivated an attempt to achieve silencing after systemic (i.v.) administration as well. After tumors were allowed to grow for 17 days, 1 mg/kg anti-luciferase siRNA or scrambled siRNA loaded DB-50B412 ternary polyplexes were injected via the tail vein on days 17, 18, and 19. A silencing effect was first detected on day 19, when the anti-luciferase group

exhibited 31% knockdown (p = 0.14) compared to the scrambled control. A statistically significant silencing effect was detected on day 20 with 44% (p = 0.04) knockdown, and the silencing was greatest at day 24 with 54% (p = 0.001) knockdown detected in anti-luciferase siRNA treated mice (Figure 8c). Efficacious in vivo gene silencing by DB-50B412 validated the functional importance of advantageous ternary polyplex design characteristics such as stability and endosomolysis of the DB core, increased cell uptake, increased blood plasma AUC, reduced renal clearance, and improved passive tumor accumulation by EPR.

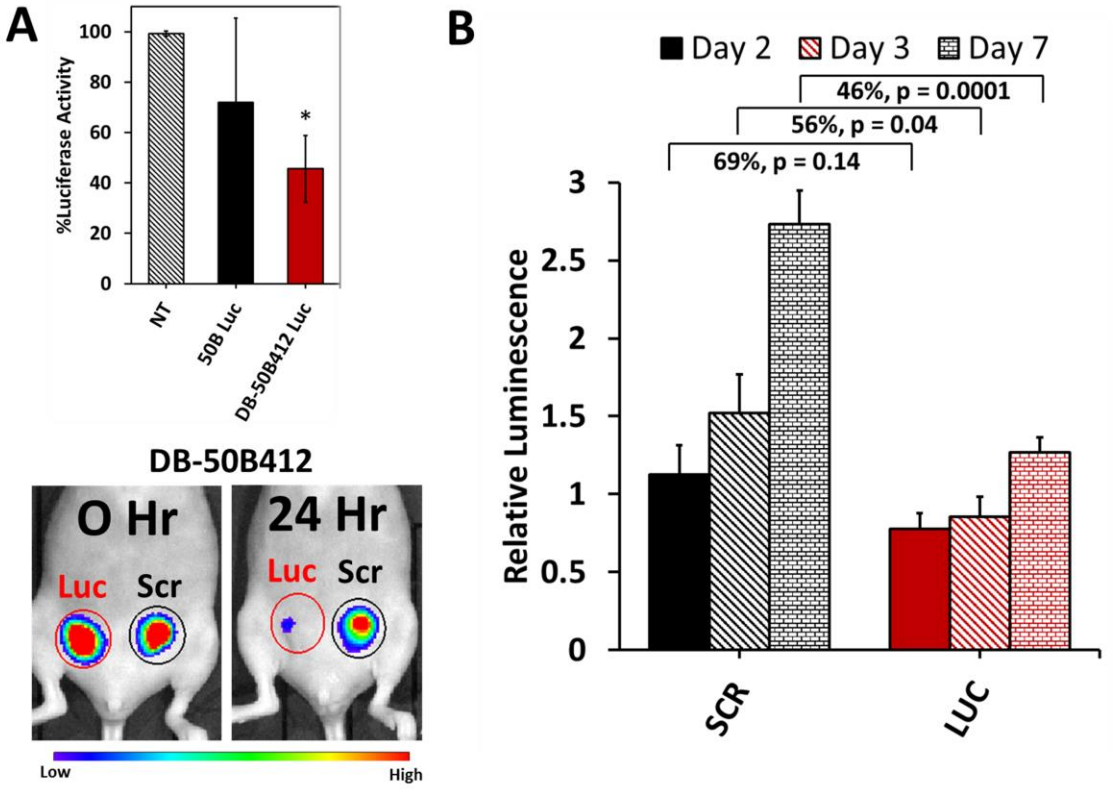

Figure 8. In vivo siRNA silencing of the model gene luciferase by ternary polyplexes. (A) Luciferase knockdown after i.t. injection of 1 mg/kg anti-luciferase siRNA, and representative images of luminescence after i.t. treatment with DB-50B412 ternary polyplexes. (C) Luciferase knockdown after i.v. injection (dosed on Day 0, 1, and 2) of 1 mg/kg anti-luciferase siRNA.

Conclusion

A combinatorial library of ternary polyplexes was developed and screened multiparametrically, providing new insights into the relative importance of various design variables for siRNA polyplexes and yielding a new siRNA nanocarrier optimized for in vivo delivery. The lead ternary polyplex, DB-50B412, had a balanced degree of PEGylation and incorporated the hydrophobically stabilized DB core-forming polymer for achieving colloidal stability with increased cell uptake, strong endosomolysis, and improved target gene silencing compared to binary polyplexes and other classes of ternary polyplexes. The DB-50B412 polyplex avoided renal clearance and stayed in circulation longer than binary polyplexes resulting in increased EPR-driven tumor accumulation. This combination of cell-level and systemic benefits led to increased in vivo gene silencing in orthotopic tumors after both local and systemic administration. Thus, our multiparametric screen successfully yielded a potent in vivo siRNA nanocarrier with validation in an orthotopic tumor model and further potential for active receptor-ligand mediated targeting to a variety of specific pathologies.

REFERENCES

1. Mislick, K.A. & Baldeschwieler, J.D. Evidence for the role of proteoglycans in cation-mediated gene transfer. *Proceedings of the National Academy of Sciences of the United States of America* **93**, 12349-12354 (1996).
2. Poon, G.M. & Gariepy, J. Cell-surface proteoglycans as molecular portals for cationic peptide and polymer entry into cells. *Biochemical Society transactions* **35**, 788-793 (2007).
3. Erbacher, P., Remy, J.S. & Behr, J.P. Gene transfer with synthetic virus-like particles via the integrin-mediated endocytosis pathway. *Gene therapy* **6**, 138-145 (1999).
4. Boussif, O. et al. A versatile vector for gene and oligonucleotide transfer into cells in culture and in vivo: polyethylenimine. *Proceedings of the National Academy of Sciences of the United States of America* **92**, 7297-7301 (1995).
5. Verbaan, F. et al. Intravenous fate of poly(2-(dimethylamino)ethyl methacrylate)-based polyplexes. *European journal of pharmaceutical sciences : official journal of the European Federation for Pharmaceutical Sciences* **20**, 419-427 (2003).
6. Kataoka, K., Harada, A. & Nagasaki, Y. Block copolymer micelles for drug delivery: design, characterization and biological significance. *Advanced Drug Delivery Reviews* **47**, 113-131 (2001).
7. Benoit, D.S., Srinivasan, S., Shubin, A.D. & Stayton, P.S. Synthesis of folate-functionalized RAFT polymers for targeted siRNA delivery. *Biomacromolecules* **12**, 2708-2714 (2011).
8. Osada, K., Christie, R.J. & Kataoka, K. Polymeric micelles from poly(ethylene glycol)-poly(amino acid) block copolymer for drug and gene delivery. *Journal of the Royal Society, Interface / the Royal Society* **6 Suppl 3**, S325-339 (2009).
9. Wakebayashi, D. et al. Lactose-conjugated polyion complex micelles incorporating plasmid DNA as a targetable gene vector system: their preparation and gene transfecting efficiency against cultured HepG2 cells. *Journal of Controlled Release* **95**, 653-664 (2004).
10. Oba, M. et al. Cyclic RGD Peptide-Conjugated Polyplex Micelles as a Targetable Gene Delivery System Directed to Cells Possessing αvβ3 and αvβ5 Integrins. *Bioconjugate chemistry* **18**, 1415-1423 (2007).
11. Nelson, C.E. et al. Balancing Cationic and Hydrophobic Content of PEGylated siRNA Polyplexes Enhances Endosome Escape, Stability, Blood Circulation Time, and Bioactivity in Vivo. *ACS Nano* **7**, 8870-8880 (2013).
12. Fire, A. et al. Potent and specific genetic interference by double-stranded RNA in Caenorhabditis elegans. *Nature* **391**, 806-811 (1998).
13. Caplen, N.J., Parrish, S., Imani, F., Fire, A. & Morgan, R.A. Specific inhibition of gene expression by small double-stranded RNAs in invertebrate and vertebrate systems. *Proceedings of the National Academy of Sciences of the United States of America* **98**, 9742-9747 (2001).
14. Elbashir, S.M. et al. Duplexes of 21-nucleotide RNAs mediate RNA interference in cultured mammalian cells. *Nature* **411**, 494-498 (2001).
15. Wang, J., Lu, Z., Wientjes, M.G. & Au, J.S. Delivery of siRNA Therapeutics: Barriers and Carriers. *AAPS J* **12**, 492-503 (2010).

16. Bartlett, D.W. & Davis, M.E. Effect of siRNA nuclease stability on the in vitro and in vivo kinetics of siRNA-mediated gene silencing. *Biotechnology and Bioengineering* **97**, 909-921 (2007).
17. Whitehead, K.A., Langer, R. & Anderson, D.G. Knocking down barriers: advances in siRNA delivery. *Nat Rev Drug Discov* **8**, 129-138 (2009).
18. Soutschek, J. et al. Therapeutic silencing of an endogenous gene by systemic administration of modified siRNAs. *Nature* **432**, 173-178 (2004).
19. Meade, B.R. et al. Efficient delivery of RNAi prodrugs containing reversible charge-neutralizing phosphotriester backbone modifications. *Nature biotechnology* **32**, 1256-1261 (2014).
20. Song, E. et al. Antibody mediated in vivo delivery of small interfering RNAs via cell-surface receptors. *Nat Biotech* **23**, 709-717 (2005).
21. Zimmermann, T.S. et al. RNAi-mediated gene silencing in non-human primates. *Nature* **441**, 111-114 (2006).
22. Dong, Y. et al. Lipopeptide nanoparticles for potent and selective siRNA delivery in rodents and nonhuman primates. *Proceedings of the National Academy of Sciences* **111**, 3955-3960 (2014).
23. Rahman, M.A. et al. Systemic delivery of siRNA nanoparticles targeting RRM2 suppresses head and neck tumor growth. *Journal of controlled release : official journal of the Controlled Release Society* **159**, 384-392 (2012).
24. Christie, R.J. et al. Targeted Polymeric Micelles for siRNA Treatment of Experimental Cancer by Intravenous Injection. *ACS Nano* **6**, 5174-5189 (2012).
25. Kanasty, R., Dorkin, J.R., Vegas, A. & Anderson, D. Delivery materials for siRNA therapeutics. *Nat Mater* **12**, 967-977 (2013).
26. Oh, Y.-K. & Park, T.G. siRNA delivery systems for cancer treatment. *Advanced Drug Delivery Reviews* **61**, 850-862 (2009).
27. Mislick, K.A. & Baldeschwieler, J.D. Evidence for the role of proteoglycans in cation-mediated gene transfer. *Proceedings of the National Academy of Sciences* **93**, 12349-12354 (1996).
28. Venkataraman, S. et al. The role of PEG architecture and molecular weight in the gene transfection performance of PEGylated poly(dimethylaminoethyl methacrylate) based cationic polymers. *Biomaterials* **32**, 2369-2378 (2011).
29. Mishra, S., Webster, P. & Davis, M.E. PEGylation significantly affects cellular uptake and intracellular trafficking of non-viral gene delivery particles. *European Journal of Cell Biology* **83**, 97-111 (2004).
30. Sato, A. et al. Polymer brush-stabilized polyplex for a siRNA carrier with long circulatory half-life. *Journal of Controlled Release* **122**, 209-216 (2007).
31. Zuckerman, J.E., Choi, C.H., Han, H. & Davis, M.E. Polycation-siRNA nanoparticles can disassemble at the kidney glomerular basement membrane. *Proceedings of the National Academy of Sciences of the United States of America* **109**, 3137-3142 (2012).
32. Naeye, B. et al. In vivo disassembly of IV administered siRNA matrix nanoparticles at the renal filtration barrier. *Biomaterials* **34**, 2350-2358 (2013).
33. Green, J.J. et al. Combinatorial Modification of Degradable Polymers Enables Transfection of Human Cells Comparable to Adenovirus. *Advanced Materials* **19**, 2836-2842 (2007).

34. Tzeng, S.Y. & Green, J.J. Subtle Changes to Polymer Structure and Degradation Mechanism Enable Highly Effective Nanoparticles for siRNA and DNA Delivery to Human Brain Cancer. *Advanced healthcare materials* **2**, 468-480 (2013).
35. Mangraviti, A. et al. Polymeric Nanoparticles for Nonviral Gene Therapy Extend Brain Tumor Survival in Vivo. *ACS Nano* **9**, 1236-1249 (2015).
36. Dahlman, J.E. et al. In vivo endothelial siRNA delivery using polymeric nanoparticles with low molecular weight. *Nat Nano* **9**, 648-655 (2014).
37. Alabi, C.A. et al. Multiparametric approach for the evaluation of lipid nanoparticles for siRNA delivery. *Proceedings of the National Academy of Sciences* **110**, 12881-12886 (2013).
38. Convertine, A.J., Benoit, D.S., Duvall, C.L., Hoffman, A.S. & Stayton, P.S. Development of a novel endosomolytic diblock copolymer for siRNA delivery. *Journal of controlled release : official journal of the Controlled Release Society* **133**, 221-229 (2009).
39. Evans, B.C. et al. Ex Vivo Red Blood Cell Hemolysis Assay for the Evaluation of pH-responsive Endosomolytic Agents for Cytosolic Delivery of Biomacromolecular Drugs. e50166 (2013).
40. Chiefari, J. et al. Living Free-Radical Polymerization by Reversible Addition−Fragmentation Chain Transfer: The RAFT Process. *Macromolecules* **31**, 5559-5562 (1998).
41. Boyer, C. et al. Bioapplications of RAFT Polymerization. *Chemical Reviews* **109**, 5402-5436 (2009).
42. Lv, H., Zhang, S., Wang, B., Cui, S. & Yan, J. Toxicity of cationic lipids and cationic polymers in gene delivery. *Journal of controlled release : official journal of the Controlled Release Society* **114**, 100-109 (2006).
43. Dash, P.R., Read, M.L., Barrett, L.B., Wolfert, M.A. & Seymour, L.W. Factors affecting blood clearance and in vivo distribution of polyelectrolyte complexes for gene delivery. *Gene therapy* **6**, 643-650 (1999).
44. Verbaan, F.J. et al. The fate of poly(2-dimethyl amino ethyl)methacrylate-based polyplexes after intravenous administration. *International journal of pharmaceutics* **214**, 99-101 (2001).
45. Tang, L. et al. Investigating the optimal size of anticancer nanomedicine. *Proceedings of the National Academy of Sciences* **111**, 15344-15349 (2014).
46. Alexis, F., Pridgen, E., Molnar, L.K. & Farokhzad, O.C. Factors affecting the clearance and biodistribution of polymeric nanoparticles. *Molecular pharmaceutics* **5**, 505-515 (2008).
47. Otsuka, H., Nagasaki, Y. & Kataoka, K. PEGylated nanoparticles for biological and pharmaceutical applications. *Advanced Drug Delivery Reviews* **64, Supplement**, 246-255 (2012).
48. Medina-Kauwe, L.K., Xie, J. & Hamm-Alvarez, S. Intracellular trafficking of nonviral vectors. *Gene therapy* **12**, 1734-1751 (2005).
49. Gilleron, J. et al. Image-based analysis of lipid nanoparticle-mediated siRNA delivery, intracellular trafficking and endosomal escape. *Nat Biotech* **31**, 638-646 (2013).
50. Kong, W.H. et al. Efficient intracellular siRNA delivery strategy through rapid and simple two steps mixing involving noncovalent post-PEGylation. *Journal of controlled release : official journal of the Controlled Release Society* **138**, 141-147 (2009).

51. Huang, Y. et al. Binary and ternary complexes based on polycaprolactone-graft-poly (N, N-dimethylaminoethyl methacrylate) for targeted siRNA delivery. *Biomaterials* **33**, 4653-4664 (2012).
52. Torchilin, V. Tumor delivery of macromolecular drugs based on the EPR effect. *Adv Drug Deliv Rev* **63**, 131-135 (2011).
53. Maeda, H., Nakamura, H. & Fang, J. The EPR effect for macromolecular drug delivery to solid tumors: Improvement of tumor uptake, lowering of systemic toxicity, and distinct tumor imaging in vivo. *Adv Drug Deliv Rev* **65**, 71-79 (2013).

APPENDIX

Supplementary Figures

Oligonucleotide	Sequence (5’ -> 3’)	Source
Alexa488-Sense	Proprietary	IDT
Alexa488-Antisense	Proprietary	IDT
Cy5-Sense	GTCAGAAATAGAAACTGGTCATC	Sigma
Cy5-Antisense	[Cyanine5]GATGACCAGTTTCTATTTCTGAC	Sigma
Luc-Sense	CAAUUGCACUGAUAAUGAACUCC[dT][dC]	Sigma
Luc-Antisense	GAGGAGUUCAUUAUCAGUGCAAUUGUU	Sigma
Scr-Sense	CGUUAAUCGCGUAUAAUACGCGU[dA][dT]	Sigma
Scr-Antisense	AUACGCGUAU[mU]A[mU]ACGCGAU[mU]A[mA]C[mG][mA][mC]	Sigma

*Nomenclature: [d] = chiral DNA base, [m] = backbone 2’O-methyl modification

Figure S1. Table of oligonucleotide sequences used throughout the studies.

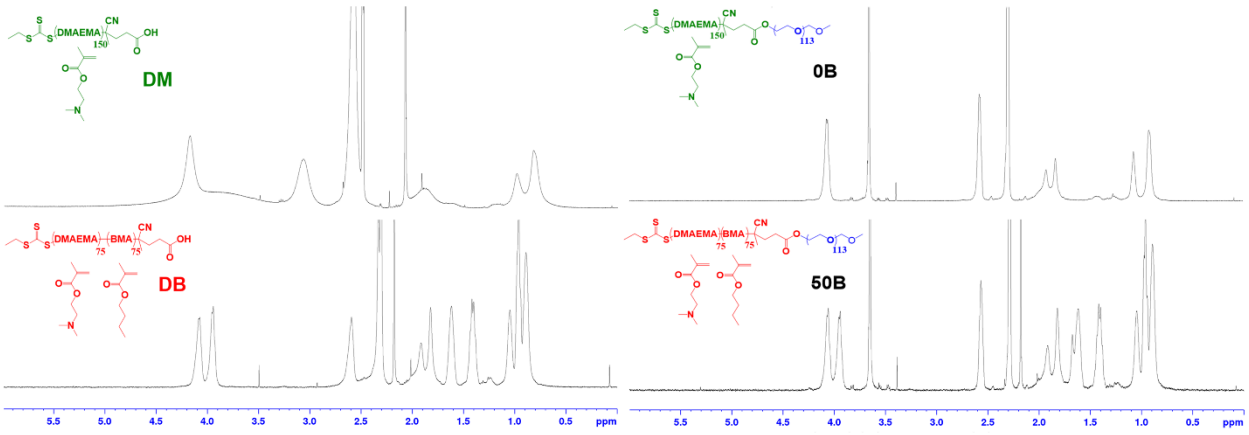

Figure S2. ^{1}H-NMR characterization of DM, DB, 0B, and 50B polymers used as base units of ternary polyplexes.

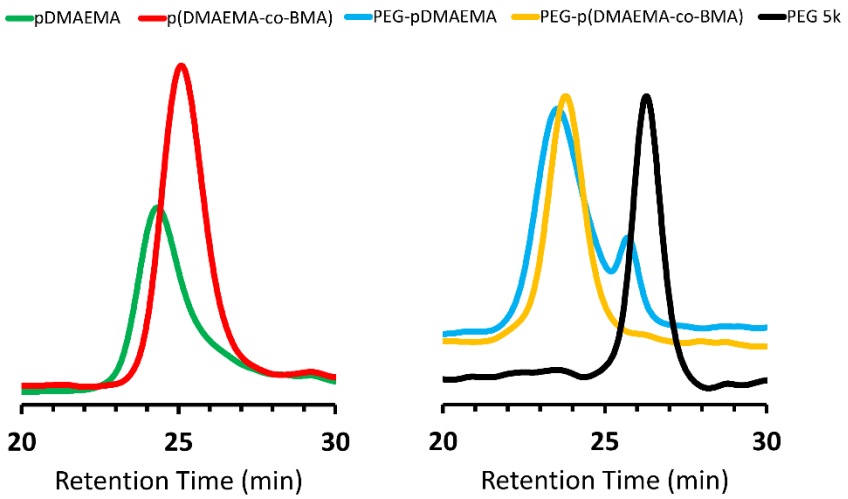

Figure S3. Gel Permeation Chromatography (GPC) elugrams of DM, DB, 0B, and 50B polymers used as the base units of ternary polyplexes.

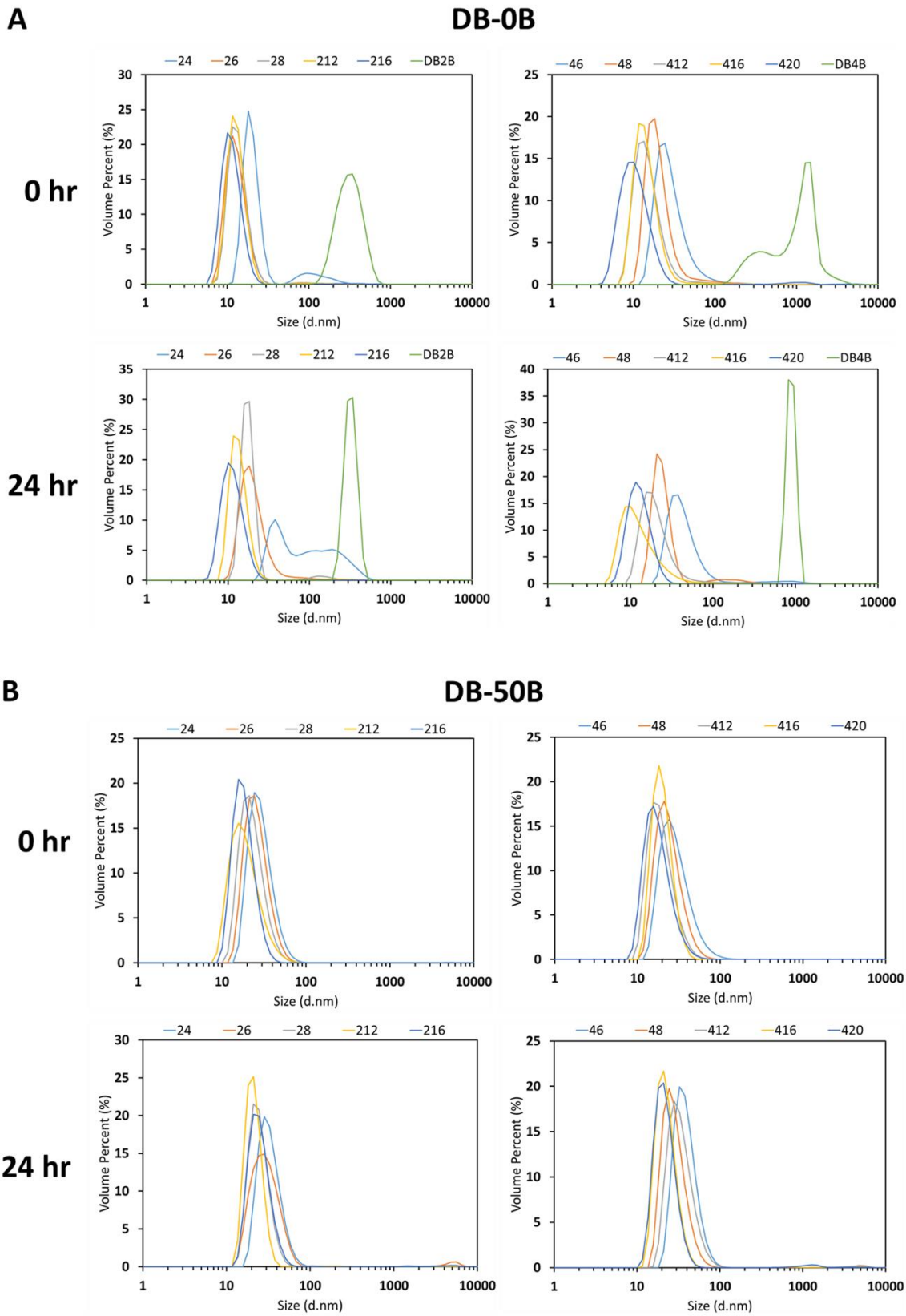
A
DB-0B
0 hr
24 hr
24
26
28
212
216
DB2B
46
48
412
416
420
DB4B
Volume Percent (%)
Size (d.nm)
B
DB-50B
0 hr
24 hr

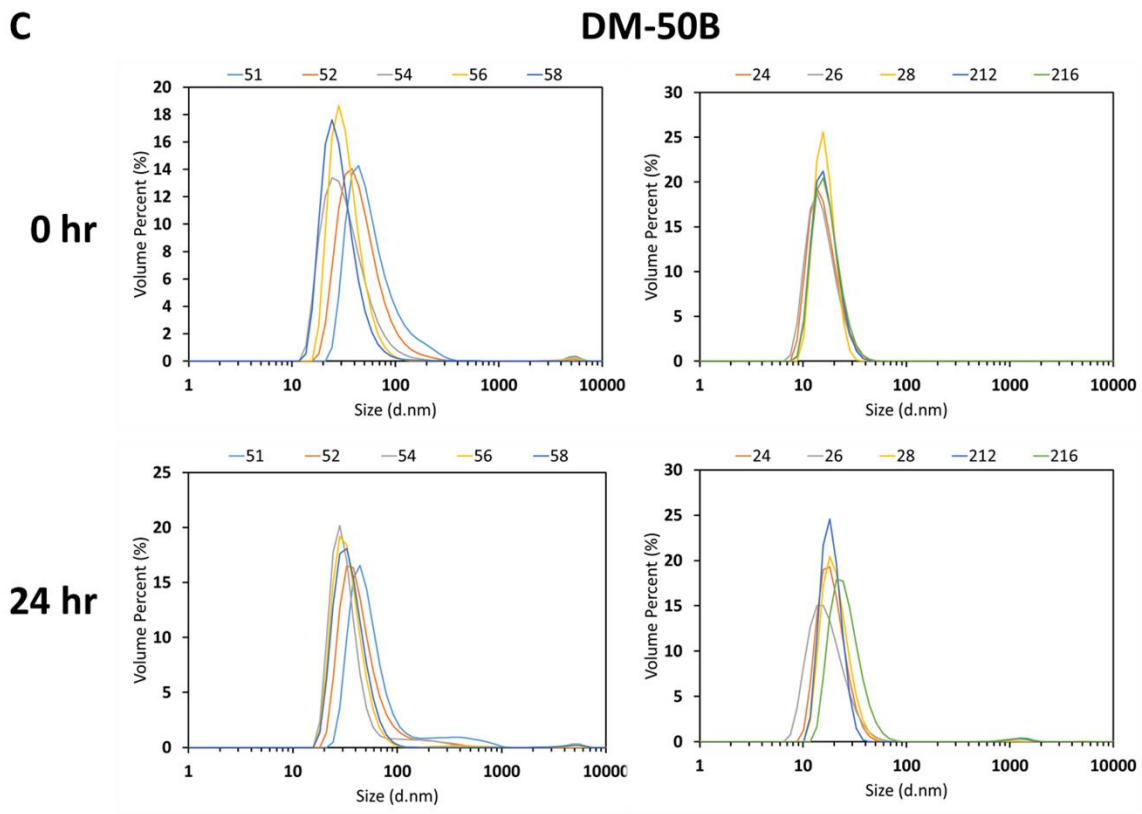

Figure S4. Comprehensive DLS spectra for (A) DB-0B, (B) DB-50B, and (C) DM-50B ternary polyplexes at 0 and 24 hr.

	DB-0B24	DB-0B26	DB-0B28	DB-0B212	DB-0B216	DB-0B46	DB-0B48	DB-0B412	DB-0B416	DB-0B420
Size - 0 Hour (nm)	19.76	13.11	13.66	13.15	11.55	31.89	23.02	17.22	15.73	10.85
Size - 24 Hour (nm)	153.8	22.39	17.42	13.67	11.64	71.84	23.95	23.17	14.49	13.2
Zeta Potential (mV)	1.27633333	1.00866667	3.36	1.86766667	0.16666667	3.19	6.01666667	4.00333333	2.21	2.453333333
	DB-50B24	DB-50B26	DB-50B28	DB-50B212	DB-50B216	DB-50B46	DB-50B48	DB-50B412	DB-50B416	DB-50B420
Size - 0 Hour (nm)	36.61	31.11	29.66	28.88	22.17	43.8	32.25	27.57	25.39	26.06
Size - 24 Hour (nm)	43.79	153.5	44.2	69.44	38	47.04	39.22	48.5	27.83	32.67
Zeta Potential (mV)	-1.7166667	-5.9466667	-4.57	-7.1566667	-3.78	-1.7633333	-3.46	-1.856	-3.31866	-9.26333333
	DM-50B51	DM-50B52	DM-50B54	DM-50B56	DM-50B58	DM-50B24	DM-50B26	DM-50B28	DM-50B212	DM-50B216
Size - 0 Hour (nm)	93.19	73.08	57.61	49.27	46.14	21.08	18.58	16.28	22.73	21.28
Size - 24 Hour (nm)	97.25	80.29	90.94	50.53	47.82	27.02	26.29	29.38	18.98	26.41
Zeta Potential (mV)	-2.8833333	-3.13	-1.0759333	0.02	-2.0896667	-1.7113333	-1.764	-0.5486667	0.151733333	-0.74466667

Figure S5. Table of DLS size (0 and 24 hr) and zeta potential values.

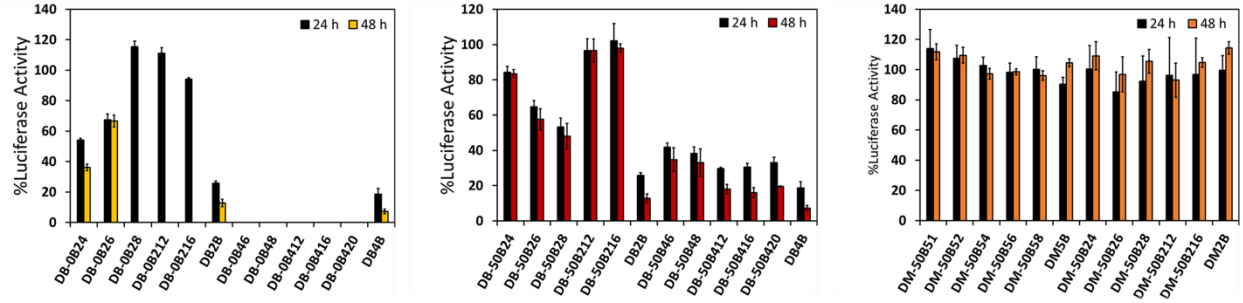

Figure S6. In vitro luciferase gene silencing by ternary polyplexes.